ijecs open access www.ijecs.in

International Journal Of Engineering And Computer Science ISSN:2319-7242
Volume 3. Issue 10 October, 2014 Page No. 8732-8740

PAPR Reduction for High-Data-Rate Through-Metal Control Network Applications Using Bit-Loaded

U.Divya Jyothi [1] L.Lakshmi Prasanna Kumar [2]

[1]Department of ECE, G Pulla Reddy College of Engineering & Technology

[2]Assistant professor, Department of ECE, G Pulla Reddy College of Engineering & Technology

ABSTRACT:

Data transmission through metallic structures is commonly needed in industrial control applications. in an exceedingly range of those applications, mechanically penetrating the structure to pass cables and establish a wired communication link is either impossible or undesirable. Examples of such structures include metal bulkheads, pressure vessels, or pipelines. Ultrasonic communication has been projected as an answer for through-metal information transfer without penetrating the structure. The reverberating nature of the through-metal channel, however, will cause significant inter-symbol interference, limiting the info rate possible by conventional single-carrier communication techniques. During this paper, we tend to describe a through-metal communication technique that exploits the slow-varying nature of the ultrasonic channel to implement AN orthogonal-frequency-division multiplexing-based rate-adaptive peak-to-average power quantitative relation (PAPR) reduction algorithm. Measurements of the projected adaptive algorithm have demonstrated transmitted output rates. This improvement provides the desired output and error rate to support high-rate network applications in otherwise data-limited environments.

INTRODUCTION

ORTHOGONAL frequency division multiplexing (OFDM) systems have been extensively applied in wireless communication systems, e.g. Worldwide Interoperability for Microwave Access (Wi MAX). It is widely known that OFDM is an attractive technique for achieving high data transmission rate in wireless communication systems and it is robust to the frequency selective fading channels [1] OFDM systems have one major disadvantage, i.e. a very high Peak-to-Average Power Ratio (PAPR) at the transmitter [2] which causes signal distortion such as in-band distortion and out-of band radiation due to the nonlinearity of the high power amplifier (HPA) and a worse bit error rate (BER) [3]. To reduce the distortions caused by the nonlinearity of HPA it requires a large backoff from the peak power which is a significant burden, especially in mobile terminals The large PAPR increases the

complexity of analog-to-digital converter (ADC) and digital-to-analog converter (DAC). Thus, PAPR reduction is one of the major problems in OFDM systems. PAPR reduction schemes can be classified according to several criteria. First, with respect to the computational operation in the frequency domain the PAPR schemes can be categorized as multiplicative and additive schemes tone reservation (TR) [5], peak canceling, and clipping [6] are additive schemes, because peak reduction vectors are added to the input symbol vector.

Extensive research has been devoted to PAPR reduction [25]–[28], including the OFDM symbol rotation and inversion algorithm provided by Tan and Bar-Ness [29]. We modify this rotation and inversion technique and apply it to the ultrasonic environment, where will further improve the effectiveness of ABL since ABL approaches attempt to maximize throughput for a given link quality. Thus, extending the work performed in [18]–[21] to address PAPR, the contribution of this paper is the demon-station of this synergistic relationship between reduced PAPR and ABL in the ultrasonic through-metal channel for the same peak transmit power [30].

Furthermore, the slow-varying nature of this particular channel easily allows for the maintenance of the channel state information (CSI) required for rate adaptation, making the algorithm computationally tractable. Unlike in conventional wireless links, this CSI remains accurate over a long duration of time and therefore enables adaptation to channel conditions with limited overhead.

The performance measurements of the proposed adaptive algorithm have demon-started increased transmitted throughput rates while maintaining low BERs at average transmit powers near 6 dBm and reducing PAPR. This performance constitutes a significant data rate improvement over conventional through-metal communication techniques while meeting acceptable quality-of-service requirements.

ULTRASONIC THROUGH - METAL CHANNEL

The ultrasonic through-metal channel is composed of the ultrasonic transducers and the metal barrier dividing them (see Fig. 1). The transmitting transducer generates acoustic waves driven by an electric voltage, and the receiving transducer converts this acoustic energy back into electric current. Primer no et al. [15] experimentally demonstrated that the ultrasonic system shown in Fig. 1 is approximately linear with respect to an ensemble of rectangular pulse tests. Thus, we can model the system as having a transient response consisting of a primary resonant pulse and a series of delayed echoes. The echoing is caused by impedance mismatch, diffraction, and transceiver misalignment. Furthermore, this echoing is responsible for intersymbol interference (ISI) when using high-rate single-carrier modulation techniques [15]. To demonstrate the severity of echoing within the ultrasonic through-metal channel, an experimentally measured frequency sweep of the channel magnitude response for 0.25-in-thick mild steel is shown in Fig. 2. Impedance mismatch at the junction between the transducer and bulkhead causes reflections at the barrier. The reflection

coefficient at this transducer–bulkhead junction is approximately -0.48 [15]. As seen in Fig. 2, deep nulls and high peaks occur within the magnitude response (i.e., it is highly frequency selective). The nulls are related to the acoustic echoing in the channel, where the spacing between nulls is equal to the reciprocal of the round-trip echo period of the channel. The physical thickness of the wall and the speed of sound in the metal determine this round-trip echo period. The frequency selectivity observed in the acoustic channel of Fig. 2 makes high-speed communication a challenge when using single-carrier modulation techniques. Additionally, the long coherence time of the channel makes it an ideal environment for adaptive algorithms. In the following sections, the authors describe an OFDM-based adaptive algorithm designed to counteract the echo-induced channel interference without excessive overhead.

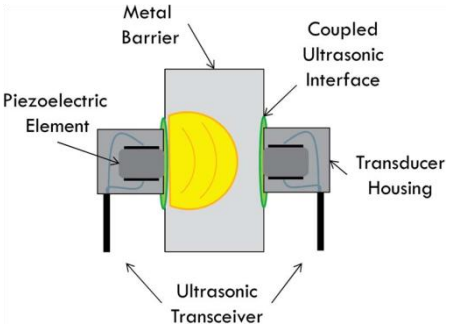

Fig 1. Through - metal channel model.

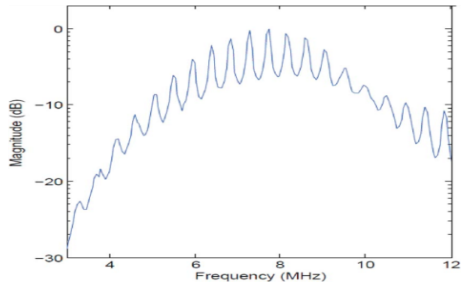

Fig.2. Through-metal channel frequency response.

II. CHARACTERIZATION OF OFDM SIGNAL

OFDM System Model

Let $\mathbf{X} = [\mathbf{X_0}\ \mathbf{X_1} \ldots \mathbf{X_{N-1}}]^T$ denote an input symbol vector in the frequency domain , where $\mathbf{X_k}$ represents the complex data of the kth subcarrier and the number of subcarriers are represented by the N. The input symbol vector is also called the input symbol sequence. Generally, an OFDM signal is the sum of independent data symbols modulated by phase-shift keying (PSK) or quadrature amplitude modulation (QAM) each of which is separated by $1/N\mathbf{t_s}$ in the frequency domain, where $\mathbf{t_s}$ is the sampling period. Then, a continuous time baseband OFDM signal is defined as

$$\mathbf{a_t} = \frac{1}{\sqrt{N}} \sum_{k=0}^{N-1} \mathbf{X_k} e^{j2\pi \frac{k}{Nt_s} t}, \qquad 0 \le t \le Nt_s$$

The discrete time base band OFDM signal $\mathbf{a_n}$ sampled at the nyquist rate $t=n\mathbf{t_s}$ can be given as

$$\mathbf{a_n} = \frac{1}{\sqrt{n}} \sum_{k=0}^{N-1} \mathbf{X_k} e^{j2\pi \frac{k}{N} n}, \qquad n = 0, 1, .. N-1$$

A discrete time OFDM signal vector denoted by $a= [\mathbf{a_0}, \mathbf{a_1}, \ldots \mathbf{a_{N-1}}]^{\ t}$. Then, **a** corresponds to the inverse fast Fourier transform (IFFT) of X , that is, **a** = QX, where Q is the IFFT matrix.

ADAPTIVE OFDM COMMUNICATION ALGORITHM

A block diagram of the adaptive OFDM-based ultrasonic through-metal communication algorithm is provided in Fig. 3. Source data bits are encoded and modulated at the transmitter in accordance with the bit distribution calculated by the ABL algorithm [19]–[21].

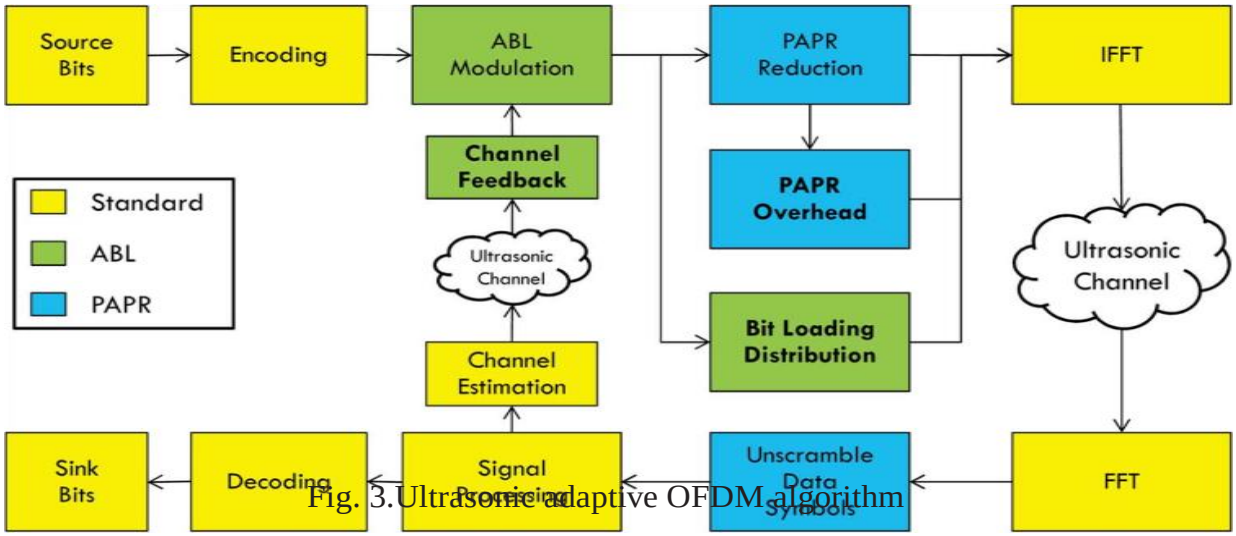

Fig. 3.Ultrasonic adaptive OFDM algorithm

The addition of a cyclic prefix to the OFDM frame is used to limit ISI from consecutive OFDM words. Assuming that each OFDM subcarrier is flat fading, the received signal of the k^{th} subcarrier

$$y_k = \sqrt{e_k}\, h_k x_k + n_k \qquad k=1,2,\ldots\ldots N$$

Where e_k is the power associated with the kth subcarrier, h_k and x_k are the kth subcarrier channel response and transmitted symbol, respectively, and nk is the additive white Gaussian noise (AWGN) of the kth subcarrier. Noise is assumed to have zero mean and unit variance, and the time index has been removed for simplicity.

The rate adaptive algorithm relies on the assumption that the transmission channel remains stationary over a minimum duration of three packets. This limitation is due to the fact that an initial non adaptive transmission must be performed to acquire the CSI at the receiver.For the ABL algorithm implemented here, this CSI is a size N array of error vector magnitudes (EVMs) calculated below for each of the k = 1,2,...,N subcarriers, where E{•} is the expectation operator

$$EVM_K = E\{|x_k - \hat{x}_k|^2\}$$

It is assumed that the CSI is accessible to the transmitter in order to determine the optimal bit loading distribution. This optimal distribution is also conveyed from the transmitter to the receiver for proper decoding. While the channel must be stationary for a minimum of three packet transmissions, the ultrasonic channel fades very slowly in practice. This slow fading reduces the need for excessive channel training and limits the channel resources dedicated to training overhead. After modulation, the PAPR is reduced through the symbol rotation and inversion algorithm by Tan and Bar-Ness [29] which finds the minimal PAPR symbol sequence upon symbol permutation in the frequency domain. Information regarding the number of rotations and inversions necessary to achieve the minimum PAPR sequence is stored and sent to the receiver, as shown in the "PAPR Overhead" block in Fig. 3.

This information is used to recover the original data sequence prior to demodulation at

the receiver. Prior to transmission, the overhead information is appended to the data stream along with the preamble and header to construct the final OFDM packet. Note that, irrespective of the ABL data rates used on the data stream, all appended information is transmitted at a low data rate to ensure reliable decoding at the receiver. The data packet is converted to the time domain via an inverse fast Fourier transform (FFT). Upon reception, the data are converted back to the frequency domain via FFT, unscrambled using the PAPR overhead, equalized, demodulated, and decoded at the receiver. Additional details of the ABL and PAPR reduction techniques used in the proposed algorithm are described.

A. ABL

ABL algorithm attempts to increase the number of bits per OFDM symbol under a fixed energy and BER constraint. This algorithm is based on the signal-to-noise ratio (SNR) "gap," it provides an estimate of the additional power necessary for transmission using discrete constellations when compared to capacity-achieving Gaussian codebooks [32]. The gap concept relates the receiver SNR to a desired symbol error rate under the assumption of equally probable messages. The ultrasonic OFDM bit loading algorithm implemented here considers the relationship between the received SNR and the bit error probability of Gray-coded square-QAM modulation through the use of the EVM of the training transmission [18]–[21]. The post processing SNR (PPSNR) for each individual subcarrier can be estimated by (5). Functions for the minimum PPSNR required to achieve a given probability of error in the range of 10−4–10−6 using even M-QAM modulation orders were formulated to generate an offline lookup table. The algorithm performs modulation order decisions by comparing the measured estimates of the subcarrier-based PSNR values to those in the lookup table such that the optimal distribution of bits among the subcarriers is allocated. If the SNR for the kth subcarrier is less than that required for 4-QAM, binary phase shift keying (BPSK) is selected as the default modulation order

$$PSNR_k = \frac{E\{|x_k|^2\}}{EVM_k}$$

Additional bit loading algorithms created by Campello [33] it computes the energy-tight bit distributions. This concept of tightening energy further optimizes ABL so that no other bit distribution can be calculated across all subcarriers such that an equivalent number of bits can be loaded with less average energy within the individual symbols. To ensure that the subcarriers remain energy tight, power scaling of the individual subcarriers is performed. So in the proposed algorithm that two variations of ABL have been developed. The power-scaled rate adaptive (PSRA) variation is similar to those energy-tight algorithms developed by Campello [33], while the non-PSRA (NPSRA) algorithm does not scale power. But the NPSRA algorithm it does not make efficient use of subcarrier symbol energy so this algorithm is suboptimal Rather, the NPSRA variation assumes average unit power across all subcarriers. 2) Successive Suboptimal Combined Symbol Rotation and Inversion Algorithm: The suboptimal approach to PAPR reduction discussed by Tan and Bar-Ness [29] is named the successive suboptimal combine symbol

rotation and inversion (SS-CSRI) algorithm. In contrast to the O-CSRI implementation, the minimal PAPR is found successively—the random permutations are performed within each individual block (while keeping the other blocks the same) rather than performing permutations across all blocks. so, the N complex symbols are first divided into blocks of (N/M) elements, as was done in the optimal approach. Next, symbol rotation and inversion is performed on only the first of M blocks for a total of (2N/M) sequences in the first block. The combination with the smallest PAPR in the first block is stored. Computational Complexity: In the optimal approach (O-CSRI), the number of possible sequences grows exponentially with N, assuming that the number of symbols in each block is constant. Thus, for large M, a significant number of comparisons is needed in order to locate the sequence with minimal PAPR. Complexity becomes prohibitively high and makes this approach impractical. However, the suboptimal algorithm (SS-CSRI) limits the total number of combinations to 2N. Although the search space for the minimal PAPR is significantly reduced, the suboptimal algorithm still offers high performance [29]. Table I demonstrates the complexity reduction achieved by using the suboptimal approach when N = 512 subcarriers and M = 16 blocks are considered. It should be mentioned that, despite the reduction of permutations performed by the suboptimal algorithm, the amount of overhead necessary to decode the original OFDM sequence at the receiver is the same as that in the optimal approach, namely, M $\log_2$ (2N/M).

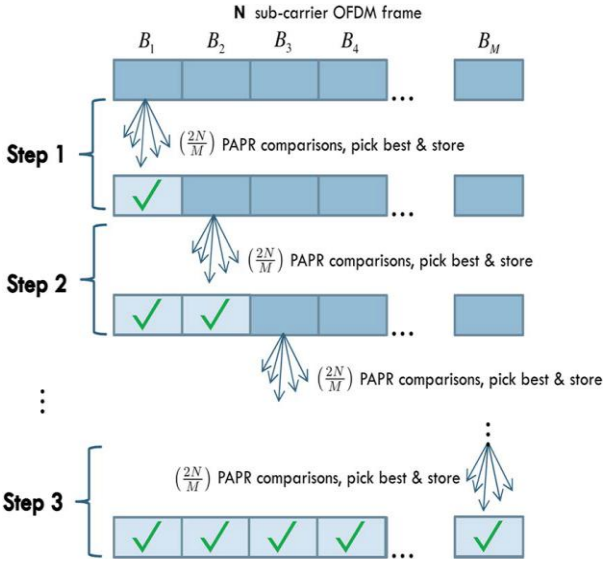

Fig. 4. Successive selection of minimal PAPR on a block-by-block basis in SS-CSRI algorithm.

COMPARISON OF ALGORITHM COMPLEXITY

COMPARISSON OF ALGORITHM COMPLEXITY

Optimal (OCSRI)	SUB-optimal (SS-CCSRI)
$\left(\frac{2N}{M}\right)\ldots\left(\frac{2N}{M}\right) = \approx 7.93x10^{28}$	$\left(\frac{2N}{M}\right)\ldots\left(\frac{2N}{M}\right) = 2N$
M	1024

The same amount of overhead is necessary in both approaches because the number of times that the symbols were rotated (as well as whether they were inverted or not) needs to be conveyed.

C. Novel PAPR-Reduction ABL Algorithm

Modifications must be made to the SS-CSRI algorithm to combine PAPR reduction and ABL techniques into a unified algorithm, as the original algorithm was not designed to work in the context of subcarrier-based modulation. A comparison of the modified algorithm and the

original SS-CSRI algorithm is therefore provided in Fig. 6. Unlike the conventional SS-SCRI algorithm, M is determined by the number of modulation orders selected by the ABL algorithm to transmit the OFDM sequence. For example, if the ABL algorithm determines that the optimal bit distribution uses a combination of BPSK, 4-QAM, and 16-QAM, the number of divisions, M, is 3. Dividing the OFDM sequence into the same number of blocks as modulation orders ensures that only data symbols of the same modulation order may be rotated and inverted. Since the blocks depend on channel conditions and vary in size, a check is performed to limit permutation when the number of blocks for a given modulation order is small. This avoids redundant permutation while still ensuring that the total number of permutations is maintained. Assuming a range of M modulation orders and fixed number of permutations to be performed, Np, the modified algorithm will first find the maximum permutations possible, Kmax, for the modulation order allocated to the smallest number of subcarriers. This algorithm then finds Kmax for the modulation order with the next smallest number of allocated subcarriers.

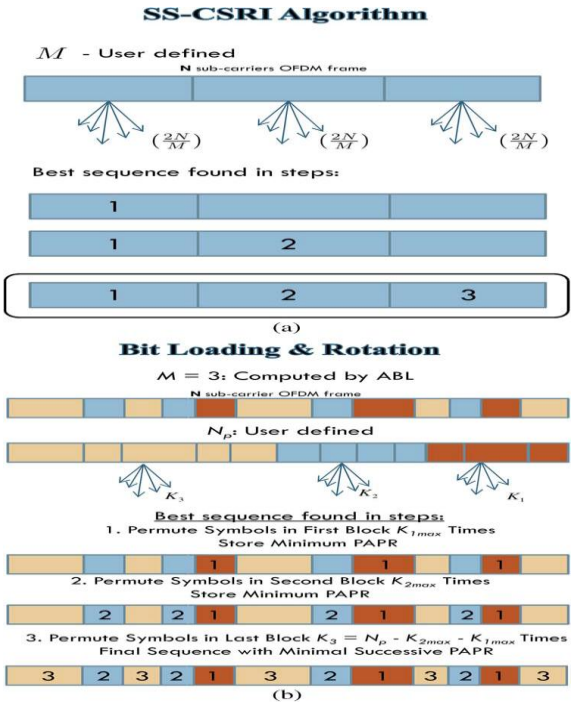

Fig. 5. Comparison of SS-CSRI and adaptive algorithms. (a) Minimal PAPR selection in SS-CSRI algorithm. (b) Minimal PAPR selection in adaptive algorithm.

This process will continue for the remaining M − 2 modulation orders. The final modulation order will then consist of $\sum_{i}^{M-1} \text{Kmaxi}$ permutations such that Np is the desired total number of permutations.

To demonstrate the steps of the modified PAPR-reduction algorithm, a small example is provided. In this example it assumed that Np = 90 and three modulation orders, BPSK,4-QAM, and 16-QAM, are used..Let assume if the number of subcarriers allocated to each modulation rate is 41, 4, and 3, respectively [30]. Then, perform the following.

1) Find Kmax for 16-QAM. With three subcarriers, a total of 3! = 6 permutations is possible.

2) Find Kmax for 4-QAM. With four subcarriers, a total of 4! = 24 permutations is possible.

3) The remaining 90 − 6 − 24 = 60 permutations are performed on subcarriers using BPSK-modulated data.

For the adaptive algorithm implementation with fixed per-mutations, N_p, the amount of control overhead necessary is M $\log_2$ (N_p /M) bits, rather than the M $\log_2$(2N/M) bits required in the original SS-CSRI implementation.

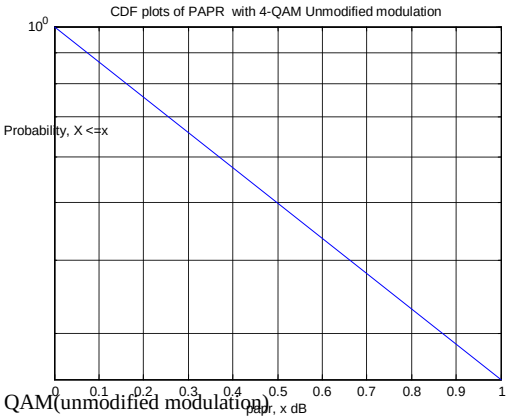

Figure 1 CDF plots with 4 QAM(unmodified modulation)

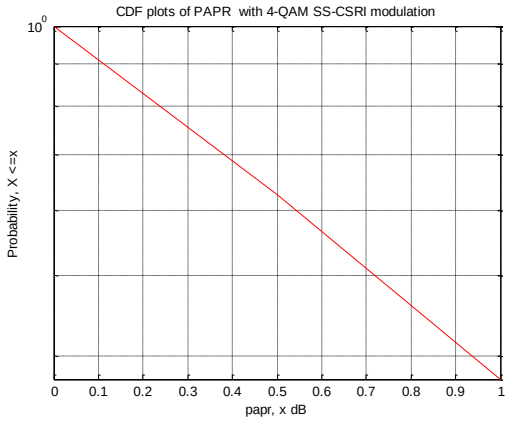

Figure 2 CDF plots with 4 QAM(SS-CSRI modulation)

SIMULATION RESULTS

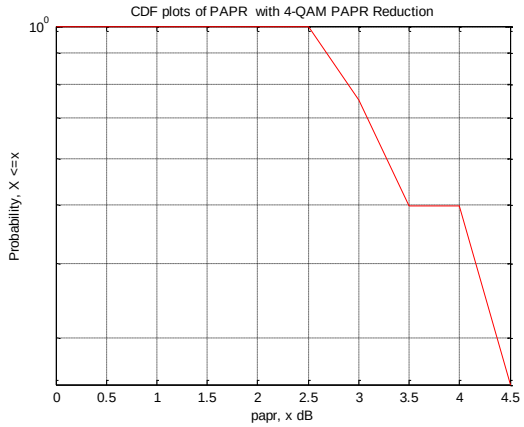

Figure 3 CDF plots with 4 QAM (PAPR reduction)

CONCLUSION:

Control network applications require data transfer through bronze structures while not penetrating the metal obstruction. Ultrasonic through-metal communication is usually employed in such environments. However, current single-carrier communication techniques area unit limited in these ultrasonic through-metal channel applications owing to acoustic echoing among the bronze barrier. OFDM will greatly improve data output in ultrasonic non penetrating through-metal communication links. Further output improvement is achieved by increasing the spectral efficiency through subcarrier-based rate accommodative algorithms and exploiting the slow-varying nature of this particular channel that simply allows for the maintenance of the CSI needed for rate adaptation. To deal with high PAPR and create additional efficient use of transmission hardware, a symbol rotation and inversion PAPR-reduction rule is modified and implemented within the adaptive OFDM framework. based on measured results, this adaptive algorithmic rule is capable of increasing data rates by roughly 280% compared

to standard single-carrier techniques at average transmit powers of roughly 6 dBm. These results provide robust proof that the bottle-neck result of using ultrasound links in wireless networks are often mitigated to lead to networks which will support higher data rate applications.

REFERENCES

[1] D. Graham, J. Neasham, and B. Sharif, "Investigation of methods for data communication and power delivery through metals," *IEEE Trans. Ind. Electron.*, vol. 58, no. 10, pp. 4972–4980, Oct. 2011.

[2] V. Gungor and G. Hancke, "Industrial wireless sensor networks: Chal-lenges, design principles, and technical approaches," *IEEE Trans. Ind. Electron.*, vol. 56, no. 10, pp. 4258–4265, Oct. 2009.

[3] K. Al Agha, M.-H. Bertin, T. Dang, A. Guitton, P. Minet, T. Val, and J.-B. Viollet, "Which wireless technology for industrial wireless sensor networks? The development of OCARI technology," *IEEE Trans. Ind. Electron.*, vol. 56, no. 10, pp. 4266–4278, Oct. 2009.

[4] Y. Ishii, "Exploiting backbone routing redundancy in industrial wireless systems," *IEEE Trans. Ind. Electron.*, vol. 56, no. 10, pp. 4288–4295, Oct. 2009.

[5] B. Lu and V. Gungor, "Online and remote motor energy monitoring and fault diagnostics using wireless sensor networks," *IEEE Trans. Ind. Electron.*, vol. 56, no. 11, pp. 4651–4659, Nov. 2009.

[6] J. Chen, X. Cao, P. Cheng, Y. Xiao, and Y. Sun, "Distributed collabora-tive control for industrial automation with wireless sensor and actuator networks," *IEEE Trans. Ind. Electron.*, vol. 57, no. 12, pp. 4219–4230, Dec. 2010.

[7] H. Sakuma, K. Nakamura, and S. Ueha, "Two-way communication over gas pipe-line using multicarrier modulated sound waves with cyclic fre-quency shifting," *Acoust. Sci. Technol.*, vol. 27, no. 4, pp. 225–232, 2006.

[8] P. Cheng, J. Chen, F. Zhang, Y. Sun, and X. Shen, "A distributed TDMA scheduling algorithm for target tracking in ultrasonic sensor networks," *IEEE Trans. Ind. Electron.*, vol. 60, no. 9, pp. 3836–3845, Sep. 2013.

[9] R. Luo and O. Chen, "Mobile sensor node deployment and asynchronous power management for wireless sensor networks," *IEEE Trans. Ind. Electron.*, vol. 59, no. 5, pp. 2377–2385, May 2012.

[10] Y. Hu, X. Zhang, J. Yang, and Q. Jiang, "Transmitting electric en-ergy through a metal wall by acoustic waves using piezoelectric transducers," *IEEE Trans. Ultrason., Ferroelectr., Freq. Control*, vol. 50, no. 7, pp. 773–781, Jul. 2003.

[11] K. Wanuga, D. Dorsey, R. Primerano, and K. R. Dandekar, "Hybrid ultrasonic and wireless networks for naval control applications," in *Proc. ASNE Intell. Ships Symp. VII*, 2007.

[12] G. Saulnier, H. Scarton, A. Gavens, D. Shoudy, T. Murphy, M. Wetzel, S. Bard, S. Roa-Prada, and P. Das, "Through-wall communication of low-rate digital data using ultrasound," in *Proc. IEEE Ultrason. Symp.*, 2006, pp. 1385–1389.